Letter

Stabilization mechanism for many-body localization in two dimensions

D. C. W. Foo [1,*] N. Swain [1,2] P. Sengupta [1,3] G. Lemarié [2,4,5] and S. Adam [1,6,7,8,†]

[1]*Centre for Advanced 2D Materials, National University of Singapore, 6 Science Drive 2, Singapore 117546*
[2]*MajuLab, International Joint Research Unit IRL 3654, CNRS, Université Côte d'Azur, Sorbonne Université, National University of Singapore, Nanyang Technological University, Singapore*
[3]*School of Physical and Mathematical Sciences, Nanyang Technological University, 21 Nanyang Link, Singapore 637371*
[4]*Centre for Quantum Technologies, National University of Singapore, Singapore 117543*
[5]*Laboratoire de Physique Théorique, Université de Toulouse, CNRS, UPS, Toulouse, France*
[6]*Department of Materials Science and Engineering, National University of Singapore, 9 Engineering Drive 1, Singapore 117575*
[7]*Yale-NUS College, 16 College Avenue West, Singapore 138527*
[8]*Department of Physics, Faculty of Science, National University of Singapore, 2 Science Drive 3, Singapore 117542*

(Received 18 February 2022; revised 7 October 2022; accepted 15 June 2023; published 20 July 2023)

Experiments in cold-atom systems see almost identical signatures of many-body localization (MBL) in both one-dimensional ($d = 1$) and two-dimensional ($d = 2$) systems despite the thermal avalanche hypothesis showing that the MBL phase is unstable for $d > 1$. Underpinning the thermal avalanche argument is the assumption of exponential localization of local integrals of motion (LIOM). In this Letter we demonstrate that the addition of a confining potential—as is typical in experimental setups—allows a noninteracting disordered system to have superexponentially (Gaussian) localized wave functions, and an interacting disordered system to undergo a localization transition. Moreover, we show that Gaussian localization of MBL LIOM shifts the quantum avalanche critical dimension from $d = 1$ to $d = 2$, potentially bridging the divide between the experimental demonstrations of MBL in these systems and existing theoretical arguments that claim that such demonstrations are impossible.

DOI: 10.1103/PhysRevResearch.5.L032011

Introduction. The study of disordered systems has borne rich discussion and novel phenomena ever since Anderson's seminal work [1] and the subsequent theoretical observation that *all* single-particle eigenstates of noninteracting systems of the orthogonal universality class in one and two dimensions (1D and 2D) are localized in the presence of disorder [2]. Of particular interest in recent years is the phenomenon of many-body localization (MBL), wherein strong disorder drives localization of the entire eigenspectrum in the presence of interactions. MBL has since been subject to intense investigation due to both fundamental and practical reasons [3–7]. While its existence in 1D was previously accepted because of good agreement among numerical [8–11], analytical [12], and experimental [13,14] work, more recently, some authors have cast doubt on the stability of the $d = 1$ MBL state in the thermodynamic limit [15–20]. As we discuss below, our results here push these concerns from $d = 1$ to $d = 2$; in particular, we show a mechanism to make MBL in $d = 1$ stable to thermal avalanches.

The situation in 2D however has always been contentious. On one hand, experimental [21,22] and numerical [23–28] signatures of MBL in 2D are almost identical to those in 1D [13], but on the other the thermal avalanche hypothesis (TAH) [29,30] posits that MBL cannot exist in any system of dimension greater than 1. The leading justification states the accessible system sizes/timescales are insufficient to observe avalanches. Without prejudice to these prior explanations, we note that the TAH relies strongly on the exponential localization of local integrals of motion (LIOM) [12,31,32], an assumption that, as we show below, may be broken on more careful treatment of the disordered potential in these many-body systems.

In this Letter, we show that a confining potential, typically present in cold-atom experiments [21,22,33], affects the MBL transition by stabilizing the localized phase. We argue that this is a consequence of superexponential localization mediated by the confining potential.

We begin with a brief overview of the TAH, noting in particular the main assumption to break to allow MBL in 2D. We then present evidence of superexponential (Gaussian) localization in the noninteracting picture. Using exact diagonalization (ED) of interacting spinless fermion Hamiltonians in a disordered cosine trap, we show how such a trap promotes localization, in defiance of the TAH. Finally, we use quantum Monte Carlo (QMC) and the eigenstate-to-Hamiltonian construction (EHC) to reverse-engineer Hamiltonians hosting 2D MBL and find that a nonzero trap term spontaneously

*c2ddfcw@nus.edu.sg
†shaffique.adam@yale-nus.edu.sg

emerges. Our work challenges the commonly accepted view that thermal avalanches always destroy MBL in 2D.

Thermal avalanche hypothesis. In sufficiently large systems with uncorrelated disorder, it is inevitable for a region of locally weak disorder to emerge. These rare regions may host "thermal bubbles," which are well described by the eigenstate thermalization hypothesis (ETH) [34,35]. At the interface between localized and thermal regions, interactions between the thermal bubble and individual LIOM may thermalize those LIOM, incorporating them into the bubble. The situation is highly asymmetric and the reverse, viz., LIOM's localizing the thermal bubble, rarely happens [36]. The energy scales governing this thermalization are the bubble-LIOM matrix element $\Gamma = V\sqrt{\delta\rho}$ and the bubble level spacing δ, where V is the interaction strength and ρ is the bubble spectral function, with the thermalization of the spin proceeding if $\Gamma \gg \delta$ [29,37]. The interaction decays in accordance with the decay (localization) of LIOM through the relation $V_{ij} \sim |\psi_i\psi_j|^2 \sim \exp(-2|i-j|/\xi)$, where ψ_i is the LIOM at site i and ξ is the localization length.

Every additional LIOM incorporated into the thermal bubble halves the level spacing, so δ decays exponentially with the number of thermalized spins. The number of thermalized spins grows algebraically with the bubble size R, as $2AR^d$, and so δ decays with R as $\delta(R) = \delta_0^{-2AR^d}$, where δ_0 is the bare bubble spacing, A is a positive geometric constant and d is the system dimension. The thermal avalanche is thus driven by the ever-decreasing bubble level spacing while being limited by the bubble-LIOM interaction strength. Assuming a form $V(R) = V_0 \exp[-(R/\xi)^a]$ for the interaction, where a is a shape parameter, and that the bubble spectral function does not change dramatically with R, the criterion for avalanche propagation at a distance R from a thermal bubble in 2D is $\exp[AR^2 - (R/\xi)^a] \gg 1$ [29,30,38]. We omit a dimensionless prefactor involving a comparison of energy scales. The original formulation [29] set $a = 1$ as the authors assumed exponentially localized LIOM, and therefore an exponentially decaying coupling between the thermal bubble and LIOM.

The study of the TAH and the MBL-ETH transition has grown beyond the simple argument described above, with a wealth of numerical and analytical studies discussing, for example, Kosterlitz-Thouless scaling near the critical point [37], localization of the critical point itself [39], coexistence of localized and thermal regions [40], and the dynamical and transport properties [41,42]. However, these build upon the basic description above with the same assumption of $a = 1$.

The phase diagram derived from the avalanche condition in 2D is shown in Fig. 1. Due to the R dependence of the avalanche criterion and the implicit assumption of exponential localization, $a = 1$, it has been argued that thermal avalanches unequivocally destroy MBL in 2D, as the left-hand side increases without bound beyond a critical R^* for $a < 2$. However, exponential localization, $a = 1$, relies on assumptions that may be broken in real experiments. For example, we argue here that the presence of a trap potential likely alters the localization profiles to be Gaussian, $a = 2$. Such a change of shape qualitatively changes the behavior of the criterion in 2D, giving rise to a critical ξ^* below which thermal avalanches cannot propagate and therefore cannot destroy MBL. This

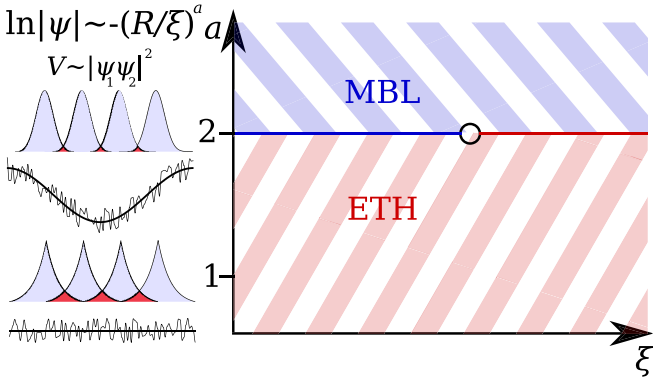

FIG. 1. The thermal avalanche hypothesis phase diagram in two dimensions for the many-body localization to eigenstate thermalization hypothesis transition as a function of localization length ξ and the local integral of motion (LIOM) shape parameter a, where $a = 2$ is critical. LIOM shapes (shaded blue) at $a = 1$ and $a = 2$ are shown on the left, with sample localization potentials (black lines) producing those LIOM shown below each. The confining potential is shown along with the total potential as a guide to the eye. The overlap of adjacent states (shaded red) highlights the qualitative difference between Gaussian and exponential localization of the LIOM. For $a < 2$, avalanches always destroy MBL, while for $a > 2$, avalanches cannot propagate. At $a = 2$, a critical ξ appears (open circle) below which MBL is stable.

completely protects MBL against thermal avalanches in $d = 1$, sidestepping recent controversy concerning the existence of MBL and moves the critical dimension up to $d = 2$.

Superexponential localization. The concept of exponentially localized LIOM is rooted in two related arguments: first in the Furstenberg theorem [43], which is most applicable in 1D, and second in the forward-scattering approximation to the locator expansion [1,4,12,44,45] which can be seen as a mean-field approximation that is more accurate in higher dimensions. Both arguments consider the joint distribution of a product of independent and identically distributed (IID) elements, coming to the conclusion that a Lyapunov exponent naturally emerges characterizing the exponential localization of a state.

The natural question therefore is what happens when these elements are not IID but correlated, as in experiments where the single-particle on-site energy consists of both disorder and confining potential terms [21,22,33]. This observation opens the possibility of new types of localization and thus the question of what effect the confining potential may have on the localization is of vital importance.

To investigate the possibility of superexponential localization numerically, we solve the 2D Anderson tight-binding model with a confining potential,

$$H_0 = -\sum_{\langle \mathbf{i},\mathbf{j}\rangle} c_{\mathbf{i}}^\dagger c_{\mathbf{j}} + \sum_{\mathbf{i}} (w_{\mathbf{i}} + V_{\mathbf{i}}) n_{\mathbf{i}}, \tag{1}$$

where $c_{\mathbf{i}}^\dagger$ ($c_{\mathbf{i}}$) creates (annihilates) a spinless fermion at site $\mathbf{i} = (i_x, i_y)$, $n_{\mathbf{i}}$ is the number operator, L is the number of sites in the linear dimension, $w_{\mathbf{i}}$ is the disordered on-site potential uniformly drawn from $[-W, W]$ and $V_{\mathbf{i}} = \frac{V_0}{4}[\cos(\frac{2\pi i_x}{L}) + \cos(\frac{2\pi i_y}{L})]$ is the confining potential. Angle brackets denote

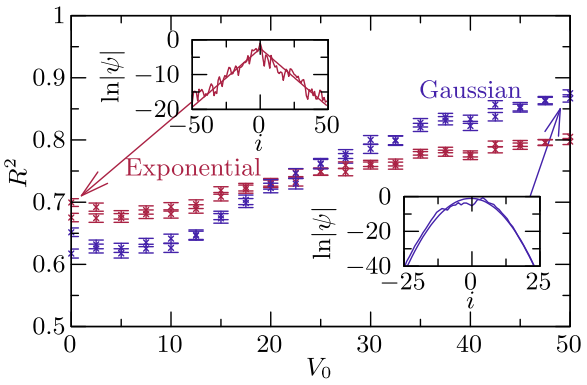

FIG. 2. Plot of the coefficient of determination R^2 when fitting the absolute value of the state closest to the spectrum center, $|\psi|$, to an exponential (red) or a Gaussian (blue) as the depth of a confining potential V_0 is increased. Two sets of data are shown to show the fit done in orthogonal directions. A clear evolution from exponential to Gaussian localization on increasing V_0 is observed. Insets: Sample $\ln|\psi|$ (solid line) and fitting function (dashed line) for $V_0 = 0$ (left, red) and $V_0 = 50$ (right, blue).

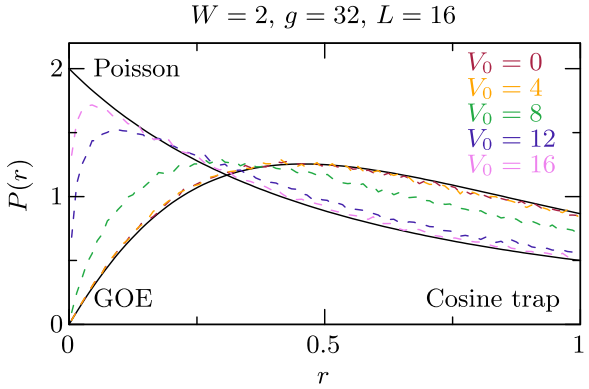

FIG. 3. Plot of the distribution $P(r)$ of level spacing ratios r for an atomic gas in a cosine trap as trap depth is increased. At $V_0 = 0$, the system thermalizes despite disorder due to strong, long-range interactions, resulting in a $P(r)$ consistent with the GOE. As V_0 increases, the system undergoes a localization transition leading to level repulsion and a Poissonian $P(r)$.

nearest neighbors (NN), and we impose periodic boundary conditions (PBCs) on both directions. The hopping term sets the energy scale, and we use $W = 5$. We use PBCs to limit finite-size effects, particularly in the interacting Hamiltonian of later sections where accessible system size is limited, but qualitatively identical behavior is seen with open boundary conditions.

We set $L = 100$ and look at the eigenstate closest to the center of the spectrum. For each disorder realization, we fit the wave function ψ to both exponential and Gaussian forms in the x and y directions. We then calculate the coefficient of determination R^2 with values closer to 1 indicating a better fit [46], and average over 400 disorder realizations. Figure 2 shows that at fixed disorder strength, as the confining potential depth V_0 increases, the wave function is better described as having a Gaussian envelope than an exponential one, suggesting that confining potentials may aid in localization by encouraging superexponential (Gaussian) decay of the wave functions. The W, V_0, and L dependence of the localization length is explored in the Supplemental Material [47].

Trap-mediated MBL. Having demonstrated the change of wave-function envelope in an Anderson localization context, we now turn on interactions to see how an ordered potential may affect the MBL transition. Owing to the exponential increase in the size of the Hilbert space, we first look at 1D. The Hamiltonian to be discussed is

$$H = H_0 + \frac{g}{L}\sum_{i\neq j}^{L}\left(1 - \frac{2|i-j|}{L}\right)n_i n_j, \tag{2}$$

where H_0 is given by the 1D analog of Eq. (1) with w_i uniformly drawn from $[-W, W]$, $V_i = \frac{V_0}{2}\cos(\frac{2\pi i}{L})$, and the second term on the right-hand side of Eq. (2) describes the interactions, with g the interaction strength. Infinite-range interactions are thought to suppress localization [48,49], so we use these to demonstrate the ability of confining potentials to promote localization. The model is readily generalized to higher dimensions, and we present results in 2D, as well as the derivation of the single-unit-cell interaction term from the infinite periodic system, in the Supplemental Material [47]. Equation (2) is analogous to the XXZ spin chain with additional longer-range diagonal interactions. For the XXZ spin chain with NN interactions, MBL is thought to occur when $V_0 = 0$, $g \neq 0$ at a critical $W_c \approx 7$ [8,50]. We therefore set $g = 32$, $W = 2$ to start in the delocalized phase as we investigate the effect of varying V_0.

We probe the localization transition by using ED to obtain the middle 1% of eigenenergies, repeated over 6400 disorder configurations, and use these to determine the probability distribution $P(r)$ of the ratio of successive energy gaps, $r_i = \min(\tilde{r}_i, \frac{1}{\tilde{r}_i})$ with $\tilde{r}_i = (E_{i+2} - E_{i+1})/(E_{i+1} - E_i)$. For time-reversal symmetric Hamiltonians such as Eq. (2), $P(r)$ is expected to follow the Gaussian orthogonal ensemble (GOE) in the delocalized phase and a Poisson distribution in the MBL phase [51–54]. For $V_0 \leqslant 4$, $P(r)$ closely adheres to that of the GOE before breaking away and transitioning to the Poisson distribution at higher V_0, as seen in Fig. 3. These results clearly indicate a transition from thermal to localized mediated by the trap depth.

These results bear some resemblance to previous work on Stark MBL [55–57], though we note that we use long-range interactions and work with periodic rather than open boundary conditions, and therefore in the $W = 0$, $g = 0$ limit the system does not admit localized solutions. This is in contrast to the Wannier-Stark localization that precedes Stark MBL [58,59].

Finite-size effects. An alternate probe of the MBL transition is the entanglement entropy, $S = -\mathrm{Tr}_A(\rho_A \log \rho_A)$ where $\rho_A = \mathrm{Tr}_B |\psi\rangle\langle\psi|$ is the partial density matrix of subsystem A when the entire system is in the state ψ. Subsystem B is the complement of A. The trapping potential V_i removes the "translationally symmetric" freedom to choose subsystems A and B, so we choose both to span a half period of V_i from maxima to minima. Results are shown in Fig. 4, where we average over the middle 1% or 100 eigenstates, whichever is fewer, and 6400 disorder configurations. We normalize by the Page value [60] $S_P = (L\log 2 - 1)/2$ to get a figure of merit between 0 and 1, where 0 indicates MBL and

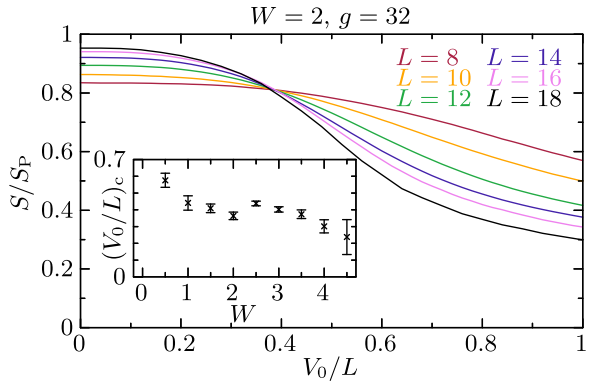

FIG. 4. Entanglement entropy of half the system against trap aspect ratio with increasing system size. Shallow traps permit a thermal phase while deep traps promote localization, with a crossover aspect ratio of $(V_0/L)_c \approx 0.37$, corresponding to a vanishing trap frequency $\omega = \pi\sqrt{V_0}/L$ in the continuum limit. The errors of the curves are within 1% and are omitted for clarity. Inset: Plot of $(V_0/L)_c$ against W. Critical potential strength is seen to decrease with increasing disorder.

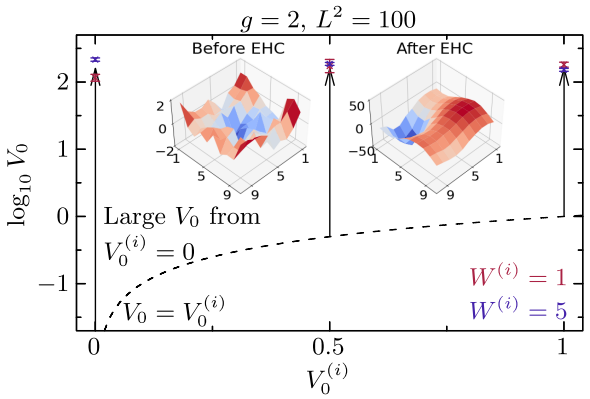

FIG. 5. MBL Hamiltonian trap depth V_0 as a function of input $V_0^{(i)}$ and $W^{(i)}$. The black dashed line indicates no change to trap depth, $V_0 = V_0^{(i)}$. V_0 is enhanced at all input $V_0^{(i)}$, particularly for $V_0^{(i)} = 0$ where a large, finite V_0 is still obtained. Insets: Sample on-site potential configurations before and after EHC for $V_0^{(i)} = 0.5$ and $W^{(i)} = 1$.

1 indicates ETH. S/S_P is plotted against the aspect ratio of the trap potential, V_0/L, for various values of L to find the transition point. The results agree with those for $P(r)$, showing a thermal to localized transition on increasing V_0 with critical aspect ratio $0.2 < (V_0/L)_c < 0.6$ for $0.5 < W < 4.5$. $(V_0/L)_c$ generally decreases with increasing W, indicating cooperation between disorder and confining potential in achieving localization.

Further insight may be obtained by considering the harmonic approximation of the confining potential about its minimum, $V_i \approx V_0(\pi i/L)^2$ for i near $L/2$. Identifying this with the quantum harmonic oscillator gives a trap frequency $\omega = \pi\sqrt{V_0}/L$ which scales as $1/\sqrt{L}$ at the critical point and thus tends to 0 in the continuum limit. These results suggest that the trap-mediated localization persists in the continuum limit.

2D numerics. ED is limited in accessible system size, so other techniques (such as QMC) are necessary to extend our numerical many-body analysis to 2D. While QMC is naively unable to target excited states, EHC [61,62] enables us to establish a mapping between input Hamiltonian $H^{(i)}$ and MBL Hamiltonian H, with H hosting the nonergodic ground state (GS) of $H^{(i)}$ as an excited state. We access the GS of $H^{(i)}$ by using an inverse temperature smaller than the finite-size gap, and thereby study excited-state properties of H. This procedure has been used to investigate MBL using QMC [28,63] and now enables us to ask the question of what trap depth V_0, if any, is needed to have nonergodic excited states, and therefore MBL. We investigate the 2D analog of Eq. (2) with NN interactions,

$$H^{(i)} = H_0 + g\sum_{\langle \mathbf{i},\mathbf{j}\rangle} n_{\mathbf{i}} n_{\mathbf{j}}, \tag{3}$$

with $w_{\mathbf{i}}$ uniformly distributed in $[-W^{(i)}, W^{(i)}]$ and $V_{\mathbf{i}} = \frac{V_0^{(i)}}{4}[\cos(\frac{2\pi i_x}{L}) + \cos(\frac{2\pi i_y}{L})]$, and obtain H via the EHC. We then calculate the autocorrelation of the on-site potential, $C_r = \sum_i U_i U_{i+r}$, where $U_i = w_i + V_i$ and extract W and V_0 from the expected form of $C_r = \frac{W^2}{3}\delta_{0,r} + \frac{V_0^2}{32L}\cos(\frac{2\pi r}{L})$.

Figure 5 shows that in general, any input $V_0^{(i)}$ maps to a much larger V_0, particularly for $V_0^{(i)} = 0$ where we always obtain a large, finite V_0. Our results indicate that a significant trap term spontaneously arises when attempting to reverse-engineer a Hamiltonian hosting 2D MBL.

Discussion and conclusions. We have revisited the TAH and noted that the underlying assumption of exponentially localized LIOM may be broken under application of trap potentials, relevant for real experiments [21,22,33], and that the localization can be made Gaussian. This observation directly challenges the assertion that MBL is generically unstable to thermal avalanches in dimension greater than 1 and opens up the possibility for stable MBL in 2D, as has previously been reported in experimental [21,22,33] and numerical [23–28] studies. The Gaussian localization length is a vanishing fraction of the trap lengthscale (see Supplemental Material [47]), indicating the applicability of our arguments to real experiments.

We have further demonstrated that the addition of a potential term to an MBL Hamiltonian may trigger an MBL transition in a parameter regime that would otherwise host a thermal phase, and that such a transition persists in the continuum limit. Nevertheless, the reader may be concerned about whether the observed stabilization of MBL in 2D are truly the result of Gaussian localization or might have some other physical origin brought on by the addition of the confining potential. Two alternative possibilities are fragmenting of the Hilbert space through emergence of new conserved quantities [64], and the rescaling of effective hopping amplitudes as the confining potential impedes particle motion. We show in the Supplemental Material [47] that neither of these explanations account for the observed localization. Our results point to external trap potentials and the concomitant Gaussian localization being the most likely stabilization mechanism for MBL in 2D and in principle able to overcome the TAH.

Potential avenues of further work include the effect of trap potentials on the dynamics of disordered systems, whether trap potentials are a viable control vector for creation and manipulation of MBL states in real time, and thus whether they may play a role in realizations of MBL-based quantum computation. Further experiments may verify stability of the MBL phase against thermal avalanches by changing the trap shape or depth. For example, a 2D system confined with a cosine potential in one direction and a square potential [65] in the orthogonal direction could give an anisotropic avalanche propagation.

Acknowledgments. The authors would like to thank Sreedevi Athira Krishnan and Kai Dieckmann for their helpful discussions and acknowledge the financial support of Singapore Ministry of Education AcRF Tier 2 Grants No. MOE2017-T2-1-130 and No. MOE2019-T2-2-118, and the Singapore National Research Foundation Investigator Award (NRF-NRFI06-2020-0003). G.L. acknowledges the support of the projects GLADYS ANR-19-CE30-0013 and MANYLOK ANR-18-CE30-0017 of the French National Research Agency (ANR), by the Singapore Ministry of Education Academic Research Fund Tier I (WBS No. R-144- 000-437-114).

[1] P. W. Anderson, Absence of diffusion in certain random lattices, Phys. Rev. **109**, 1492 (1958).
[2] F. Evers and A. D. Mirlin, Anderson transitions, Rev. Mod. Phys. **80**, 1355 (2008).
[3] I. V. Gornyi, A. D. Mirlin, and D. G. Polyakov, Interacting Electrons in Disordered Wires: Anderson Localization and Low-T Transport, Phys. Rev. Lett. **95**, 206603 (2005).
[4] D. M. Basko, I. L. Aleiner, and B. L. Altshuler, Metal-insulator transition in a weakly interacting many-electron system with localized single-particle states, Ann. Phys. **321**, 1126 (2006).
[5] R. Nandkishore and D. A. Huse, Many-body localization and thermalization in quantum statistical mechanics, Annu. Rev. Condens. Matter Phys. **6**, 15 (2015).
[6] F. Alet and N. Laflorencie, Many-body localization: An introduction and selected topics, C. R. Phys. **19**, 498 (2018).
[7] D. A. Abanin, E. Altman, I. Bloch, and M. Serbyn, Colloquium: Many-body localization, thermalization, and entanglement, Rev. Mod. Phys. **91**, 021001 (2019).
[8] D. J. Luitz, N. Laflorencie, and F. Alet, Many-body localization edge in the random-field Heisenberg chain, Phys. Rev. B **91**, 081103(R) (2015).
[9] M. Serbyn and J. E. Moore, Spectral statistics across the many-body localization transition, Phys. Rev. B **93**, 041424(R) (2016).
[10] V. Khemani, F. Pollmann, and S. L. Sondhi, Obtaining Highly Excited Eigenstates of Many-Body Localized Hamiltonians by the Density Matrix Renormalization Group Approach, Phys. Rev. Lett. **116**, 247204 (2016).
[11] S. P. Lim and D. N. Sheng, Many-body localization and transition by density matrix renormalization group and exact diagonalization studies, Phys. Rev. B **94**, 045111 (2016).
[12] J. Z. Imbrie, V. Ros, and A. Scardicchio, Local integrals of motion in many-body localized systems, Ann. Phys. **529**, 1600278 (2017).
[13] M. Schreiber, S. S. Hodgman, P. Bordia, H. P. Lüschen, M. H. Fischer, R. Vosk, E. Altman, U. Schneider, and I. Bloch, Observation of many-body localization of interacting fermions in a quasirandom optical lattice, Science **349**, 842 (2015).
[14] J. Smith, A. Lee, P. Richerme, B. Neyenhuis, P. W. Hess, P. Hauke, M. Heyl, D. A. Huse, and C. Monroe, Many-body localization in a quantum simulator with programmable random disorder, Nat. Phys. **12**, 907 (2016).
[15] J. Suntajs, J. Bonča, T. Prosen, and L. Vidmar, Quantum chaos challenges many-body localization, Phys. Rev. E **102**, 062144 (2020).
[16] P. Sierant, D. Delande, and J. Zakrzewski, Thouless Time Analysis of Anderson and Many-Body Localization Transitions, Phys. Rev. Lett. **124**, 186601 (2020).
[17] M. Kiefer-Emmanouilidis, R. Unanyan, M. Fleischhauer, and J. Sirker, Slow delocalization of particles in many-body localized phases, Phys. Rev. B **103**, 024203 (2021).
[18] P. Sierant and J. Zakrzewski, Challenges to observation of many-body localization, Phys. Rev. B **105**, 224203 (2022).
[19] D. Sels, Bath-induced delocalization in interacting disordered spin chains, Phys. Rev. B **106**, L020202 (2022).
[20] A. Morningstar, L. Colmenarez, V. Khemani, D. J. Luitz, and D. A. Huse, Avalanches and many-body resonances in many-body localized systems, Phys. Rev. B **105**, 174205 (2022).
[21] J. Choi, S. Hild, J. Zeiher, P. Schauss, A. Rubio-Abadal, T. Yefsah, V. Khemani, D. A. Huse, I. Bloch, and C. Gross, Exploring the many-body localization transition in two dimensions, Science **352**, 1547 (2016).
[22] S. S. Kondov, W. R. McGehee, W. Xu, and B. DeMarco, Disorder-Induced Localization in a Strongly Correlated Atomic Hubbard Gas, Phys. Rev. Lett. **114**, 083002 (2015).
[23] T. B. Wahl, A. Pal, and S. H. Simon, Signatures of the many-body localized regime in two dimensions, Nat. Phys. **15**, 164 (2019).
[24] A. Kshetrimayum, M. Goihl, and J. Eisert, Time evolution of many-body localized systems in two spatial dimensions, Phys. Rev. B **102**, 235132 (2020).
[25] H. Théveniaut, Z. Lan, G. Meyer, and F. Alet, Transition to a many-body localized regime in a two-dimensional disordered quantum dimer model, Phys. Rev. Res. **2**, 033154 (2020).
[26] E. Chertkov, B. Villalonga, and B. K. Clark, Numerical Evidence for Many-Body Localization in Two and Three Dimensions, Phys. Rev. Lett. **126**, 180602 (2021).
[27] K. S. C. Decker, D. M. Kennes, and C. Karrash, Many-body localization and the area law in two dimensions, Phys. Rev. B **106**, L180201 (2022).
[28] H. Tang, N. Swain, D. C. W. Foo, B. J. J. Khor, G. Lemarié, F. F. Assaad, S. Adam, and P. Sengupta, Evidence of many-body localization in 2D from quantum Monte Carlo simulation, arXiv:2106.08587.
[29] W. De Roeck and F. Huveneers, Stability and instability towards delocalization in many-body localization systems, Phys. Rev. B **95**, 155129 (2017).
[30] I.-D. Potirniche, S. Banerjee, and E. Altman, Exploration of the stability of many-body localization in $d > 1$, Phys. Rev. B **99**, 205149 (2019).

[31] M. Serbyn, Z. Papić, and D. A. Abanin, Local Conservation Laws and the Structure of the Many-Body Localized States, Phys. Rev. Lett. **111**, 127201 (2013).
[32] A. Chandran, I. H. Kim, G. Vidal, and D. A. Abanin, Constructing local integrals of motion in the many-body localized phase, Phys. Rev. B **91**, 085425 (2015).
[33] P. Bordia, H. Lüschen, S. Scherg, S. Gopalakrishnan, M. Knap, U. Schneider, and I. Bloch, Probing Slow Relaxation and Many-Body Localization in Two-Dimensional Quasiperiodic Systems, Phys. Rev. X **7**, 041047 (2017).
[34] J. M. Deutsch, Quantum statistical mechanics in a closed system, Phys. Rev. A **43**, 2046 (1991).
[35] M. Srednicki, Chaos and quantum thermalization, Phys. Rev. E **50**, 888 (1994).
[36] D. J. Luitz, F. Huveneers, and W. De Roeck, How a Small Quantum Bath Can Thermalize Long Localized Chains, Phys. Rev. Lett. **119**, 150602 (2017).
[37] P. T. Dumitrescu, A. Goremykina, S. A. Parameswaran, M. Serbyn, and R. Vasseur, Kosterlitz-Thouless scaling at many-body localization phase transitions, Phys. Rev. B **99**, 094205 (2019).
[38] W. De Roeck and J. Z. Imbrie, Many-body localization: stability and instability, Philos. Trans. R. Soc. A **375**, 20160422 (2017).
[39] T. Thiery, F. Huveneers, M. Müller, and W. De Roeck, Many-Body Delocalization as a Quantum Avalanche, Phys. Rev. Lett. **121**, 140601 (2018).
[40] P. J. D. Crowley and A. Chandran, Avalanche induced coexisting localized and thermal regions in disordered chains, Phys. Rev. Res. **2**, 033262 (2020).
[41] S. Gopalakrishnan and S. A. Parameswaran, Dynamics and transport at the threshold of many-body localization, Phys. Rep. **862**, 1 (2020).
[42] E. V. H. Doggen, I. V. Gornyi, A. D. Mirlin, and D. G. Polyakov, Slow Many-Body Delocalization beyond One Dimension, Phys. Rev. Lett. **125**, 155701 (2020).
[43] H. Furstenberg, Noncommuting random products, Trans. Am. Math. Soc. **108**, 377 (1963).
[44] D. M. Basko, I. L. Aleiner, and B. L. Altshuler, Possible experimental manifestations of the many-body localization, Phys. Rev. B **76**, 052203 (2007).
[45] F. Pietracaprina, V. Ros, and A. Scardicchio, Forward approximation as a mean-field approximation for the Anderson and many-body localization transitions, Phys. Rev. B **93**, 054201 (2016).
[46] R. G. D. Steel and J. H. Torrie, *Principles and Procedures of Statistics with Special Reference to the Biological Sciences* (McGraw-Hill, New York, 1960).
[47] See Supplemental Material at http://link.aps.org/supplemental/10.1103/PhysRevResearch.5.L032011 for details of how the localization length varies with trapping potential and system size, results for level spacing ratio calculations on 2D systems, details of the participation entropy calculations using QMC, discussion of multifractal dimension and its determination, investigations of the effect of multiple wells and other potential profiles on our results, discussion of alternate explanations involving Hilbert space fragmentation or effective hopping models, and a derivation of the periodic long-range interaction used here.
[48] R. M. Nandkishore and S. L. Sondhi, Many-Body Localization with Long-Range Interactions, Phys. Rev. X **7**, 041021 (2017).
[49] S. Nag and A. Garg, Many-body localization in the presence of long-range interactions and long-range hopping, Phys. Rev. B **99**, 224203 (2019).
[50] M. Serbyn, Z. Papić, and D. A. Abanin, Criterion for Many-Body Localization-Delocalization Phase Transition, Phys. Rev. X **5**, 041047 (2015).
[51] V. Oganesyan and D. A. Huse, Localization of interacting fermions at high temperature, Phys. Rev. B **75**, 155111 (2007).
[52] A. Pal and D. A. Huse, Many-body localization phase transition, Phys. Rev. B **82**, 174411 (2010).
[53] Y. Y. Atas, E. Bogomolny, O. Giraud, and G. Roux, Distribution of the Ratio of Consecutive Level Spacings in Random Matrix Ensembles, Phys. Rev. Lett. **110**, 084101 (2013).
[54] P. Sierant and J. Zakrzewski, Level statistics across the many-body localization transition, Phys. Rev. B **99**, 104205 (2019).
[55] M. Schulz, C. A. Hooley, R. Moessner, and F. Pollmann, Stark Many-Body Localization, Phys. Rev. Lett. **122**, 040606 (2019).
[56] S. R. Taylor, M. Schulz, F. Pollmann, and R. Moessner, Experimental probes of Stark many-body localization, Phys. Rev. B **102**, 054206 (2020).
[57] T. Chanda, R. Yao, and J. Zakrzewski, Coexistence of localized and extended phases: Many-body localization in a harmonic trap, Phys. Rev. Res. **2**, 032039 (2020).
[58] G. H. Wannier, Wave functions and effective Hamiltonian for Bloch electrons in an electric field, Phys. Rev. **117**, 432 (1960).
[59] E. P. L. van Nieuwenburg, Y. Baum, and G. Refael, From Bloch oscillations to many-body localization in clean interacting systems, Proc. Natl. Acad. Sci. USA **116**, 9269 (2019).
[60] D. N. Page, Average Entropy of a Subsystem, Phys. Rev. Lett. **71**, 1291 (1993).
[61] E. Chertkov and B. K. Clark, Computational Inverse Method for Constructing Spaces of Quantum Models from Wave Functions, Phys. Rev. X **8**, 031029 (2018).
[62] X. L. Qi and D. Ranard, Determining a local Hamiltonian from a single eigenstate, Quantum **3**, 159 (2019).
[63] M. Dupont and N. Laflorencie, Many-body localization as a large family of localized ground states, Phys. Rev. B **99**, 020202(R) (2019).
[64] J. Attig, J. Park, M. M. Scherer, S. Trebst, A. Altland, and A. Rosch, Universal principles of moiré band structures, 2D Mater. **8**, 044007 (2021).
[65] B. Mukherjee, Z. Yan, P. B. Patel, Z. Hadzibabic, T. Yefsah, J. Struck, and M. W. Zwierlein, Homogeneous Atomic Fermi Gases, Phys. Rev. Lett. **118**, 123401 (2017).